

Dynamical Localization of Bose-Einstein condensate in Optomechanics

Muhammad Ayub*,^{1,2} Kashif Ammar Yasir,¹ and Farhan Saif¹

¹*Department of Electronics, Quaid-i-Azam University, 45320, Islamabad, Pakistan.*

²*LINAC Project, PINSTECH, Nilore, 45650, Islamabad, Pakistan.*

We explain dynamical localization of Bose-Einstein condensate (BEC) in optomechanics both in position and in momentum space. The experimentally realizable optomechanical system is a Fabry-Pérot cavity with one moving end mirror and driven by single mode standing field. In our study we analyze variations in modulation strength and effective Plank's constants. Keeping in view present day experimental advances we provide set of parameters to observe the phenomenon in laboratory.

PACS numbers: 72.15.Rn, 03.75.Kk, 42.50.Pq

I. INTRODUCTION

Cavity-optomechanics deals with the interaction of an optical field in a resonator with confining mirrors [1]. Recent experimental advances make it possible to couple cold atoms and Bose-Einstein condensates (BEC), mechanical membrane and nano-sphere with the optomechanical systems [2]. Hence, these hybrid-opto mechanical systems are playground to study phenomena related to mirror-field interaction, and atom-field interaction which provide founding principles to develop numerous sensors, and devices in quantum metrology. In opto-mechanics the mechanical effects of light lead to cool the motion of a movable mirror to its quantum mechanical ground state [3–5], and to observe strong coupling effects [6–8]. In earlier work optomechanical systems were suggested to develop gravitational wave detectors [9] and to measure displacement with large accuracy [10], and in recent research work these systems lead to develop optomechanical crystals [11]. Recent theoretical discussions and simulations on bistable behavior of BEC-optomechanical system [12], high fidelity state transfer [13, 14], steady-state entanglement of BEC and moving end mirror [15], macroscopic tunneling of an optomechanical membrane [16] and role reversal between matter-wave and quantized light field are guiding towards new avenues in cavity optomechanics. In this paper, we discuss the dynamical localization of ultra-cold atoms or dilute BEC trapped inside a single mode driven optomechanical cavity with one fixed mirror and the other as a movable mirror. Dynamical localization is an interesting phenomenon in periodically driven nonlinear systems [18–22] and provides quantum mechanical limits on classical diffusion of wave packet. We show that for different modulation regimes the dynamical localization is observed both in position and in momentum space. The phenomenon of dynamical localization emerges as the hybrid optomechanical system is explicitly time dependent, hence, the single mode laser field provides spatially periodic potential to BEC with phase modulation[17] due to

modulated end mirror.

In the paper, the model of the system is presented in section II. In section III we derive the Langevin equation and in section IV, we explain dynamical localization of the condensates in the system. In section V, we explain dynamical localization as a function of modulation amplitudes. Results are summarized in section-VI.

II. THE MODEL

We consider a Fabry-Pérot cavity of length L with a moving end mirror driven by a single mode optical field of frequency ω_p and BEC with N -two level atoms trapped in an optical lattice potential [23, 24]. Moving end mirror has harmonic oscillations with frequency ω_m and exhibits Brownian motion in the absence of coupling with radiation pressure.

The Hamiltonian of BEC-optomechanical system is,

$$\hat{H} = \hat{H}_m + \hat{H}_a + \hat{H}_T, \quad (1)$$

where, \hat{H}_m describes the intra-cavity field and its coupling to the moving end mirror, \hat{H}_a accounts for the BEC and its coupling with intra-cavity field while, \hat{H}_T accounts for noises and damping associated with the system. The Hamiltonian \hat{H}_m is given as [25],

$$\hat{H}_m = \hbar\Delta_c\hat{c}^\dagger\hat{c} + \frac{\hbar\omega_m}{2}(\hat{p}^2 + \hat{q}^2) - \xi\hbar\hat{c}^\dagger\hat{c}\hat{q} - i\hbar\eta(\hat{c} - \hat{c}^\dagger), \quad (2)$$

where, first term is free energy of the field, $\Delta_c = \omega_c - \omega_p$ is detuning, here, ω_c is cavity frequency and \hat{c}^\dagger (\hat{c}) are creation (annihilation) operators for intra-cavity field interacting with mirror and condensates and their commutation relation is $[\hat{c}, \hat{c}^\dagger] = 1$. Second term represents energy of moving end mirror. Here \hat{q} and \hat{p} are dimensionless position and momentum operators for moving end mirror, such that, $[\hat{q}, \hat{p}] = i$. Intra-cavity field couple BEC and moving end mirror through radiation pressure. Third term represents such coupled energy of moving end mirror with field and $\xi = \sqrt{2}(\omega_c/L)x_0$ is the coupling strength where, $x_0 = \sqrt{\hbar/2m\omega_m}$, is zero point motion of mechanical mirror having mass m . Last term gives relation of intra-cavity field and output power

*ayubok@gmail.com

$|\eta| = \sqrt{P\kappa/\hbar\omega_p}$, where, P is the input laser power and κ is cavity decay rate associated with outgoing modes.

Now the Hamiltonian for BEC and intra-cavity field and their coupling is derived by considering quantized motion of atoms along the cavity axis in one dimensional model. We assume that BEC is dilute enough and many body interaction effects are ignored. We have

$$\hat{H}_a = \int \hat{\psi}^\dagger(x) \left(-\frac{\hbar^2}{2m_a} \frac{d^2}{dx^2} + \hbar U_0 \hat{c}^\dagger \hat{c} \cos^2 kx \right) \hat{\psi}(x) dx, \quad (3)$$

here, $\hat{\psi}(\hat{\psi}^\dagger)$ is annihilation (creation) operator for bosonic particles and $U_0 = g_0^2/\Delta_a$ is the far off-resonant vacuum Rabi frequency. Here, Δ_a is far-off detuning between field frequency and ω_0 , atomic transition frequency, m_a is mass of an atom, and k is the wave number. Due to field interaction with BEC, photon recoil takes place that generates symmetric momentum $\pm 2l\hbar k$ side modes, where, l is an integer. We assume that field is weak enough which causes low photon coupling, therefore only 0^{th} and 1^{st} order modes are excited while, higher order modes are ignored. Now $\hat{\psi}$ is depending upon these two modes [12] and defined as, $\hat{\psi}(x) = \hat{a} + \sqrt{2} \cos(2kx) \hat{b}/L$. Where, \hat{a} and \hat{b} are annihilation operators for 0^{th} and $\pm 2\hbar k^{th}$ modes respectively and are related as $\hat{a}^\dagger \hat{a} + \hat{b}^\dagger \hat{b} = N$, where, N is the number of bosonic particles. As population in 0^{th} mode is much larger than the population in 1^{st} order side mode, we write $\hat{a}^\dagger \hat{a} \simeq N$ or \hat{a} and $\hat{a}^\dagger \rightarrow \sqrt{N}$. This is possible when side modes are weak enough and for that matter can be ignored.

By using $\hat{\psi}(x)$ defined above in Hamiltonian, we write the Hamiltonian governing the field-condensate interaction as,

$$\hat{H}_a = \frac{\hbar U_0 N}{2} \hat{c}^\dagger \hat{c} + \frac{\hbar \Omega}{2} (\hat{P}^2 + \hat{Q}^2) + \xi_{sm} \hbar \hat{c}^\dagger \hat{c} \hat{Q} \quad (4)$$

here, first term describes energy of field due to the condensate. We also assume large atom-field detuning Δ_a , therefore, excited atomic levels are adiabatically eliminated. Second term expresses the energy of the condensate in the cavity following harmonic motion. Here, $\hat{P} = \frac{i}{\sqrt{2}}(\hat{b} - \hat{b}^\dagger)$ and $\hat{Q} = \frac{1}{\sqrt{2}}(\hat{b} + \hat{b}^\dagger)$ are dimensionless momentum and position operators for condensate which are related as $[\hat{Q}, \hat{P}] = i$ and $\Omega = 4\omega_r$ where, $\omega_r = \hbar k^2/2m_a$ is recoil frequency of an atom. Last term in eq. (4) describes coupled energy of field and condensate with coupling strength $\xi_{sm} = \frac{\omega_r}{L} \sqrt{\hbar/m_{sm} 4\omega_r}$, where, $m_{sm} = \hbar \omega_c^2/(L^2 N U_0^2 \omega_r)$ is the effective mass of side mode.

III. LANGEVIN EQUATIONS

The Hamiltonian \hat{H}_T accounts for the effects of dissipation in the intra-cavity field, damping of moving end mirror and depletion of BEC in the system via standard quantum noise operators [30]. The total Hamiltonian

H leads to coupled quantum Langevin equations for position and momentum of moving end mirror and BEC, viz.,

$$\begin{aligned} \frac{d\hat{c}}{dt} &= \dot{\hat{c}} = (i\tilde{\Delta} + i\xi\hat{q} - i\xi_{sm} - \kappa)\hat{c} + \eta + \sqrt{2\kappa}a_{in}, \\ \frac{d\hat{p}}{dt} &= \dot{\hat{p}} = -\omega_m\hat{q} - \xi\hat{c}^\dagger\hat{c} - \gamma_m\hat{p} + \hat{f}_B, \\ \frac{d\hat{q}}{dt} &= \dot{\hat{q}} = \omega_m\hat{p}, \\ \frac{d\hat{P}}{dt} &= \dot{\hat{P}} = -4\omega_r\hat{Q} - \xi_{sm}\hat{c}^\dagger\hat{c} - \gamma_{sm}\hat{P} + \hat{f}_{1m}, \\ \frac{d\hat{Q}}{dt} &= \dot{\hat{Q}} = 4\omega_r\hat{P} - \gamma_{sm}\hat{Q} + \hat{f}_{2m}. \end{aligned} \quad (5)$$

In above equations $\tilde{\Delta} = \Delta_c - NU_0/2$, whereas \hat{a}_{in} is Markovian input noise of the cavity field. The term γ_m gives mechanical energy decay rate of the moving end mirror and \hat{f}_B is Brownian noise operator [31]. The term γ_{sm} represents damping of BEC due to harmonic trapping potential which effects momentum side modes while, \hat{f}_{1M} and \hat{f}_{2M} are the associated noise operators assumed to be Markovian.

The coupled equations of motion which govern the dynamics of the moving end-mirror and the BEC are quantum Langevin equations (5). In adiabatic approximation we consider no thermal excitation, for the reason, we ignore noises and radiation effects resulting from optical damping [1, 24, 32]. Therefore, in short time limit we ignore the mechanical damping, as a result the coupled equations of motion for the moving end-mirror and BEC reveal their coupled nonlinear oscillator dynamics, that is,

$$\frac{d^2\hat{q}}{dt^2} = -\omega_m^2\hat{q} + \frac{\omega_m\xi\eta^2}{\kappa^2 + (\tilde{\Delta} + \xi\hat{q} - \xi_{sm}\hat{Q})^2}, \quad (6)$$

$$\frac{d^2\hat{Q}}{dt^2} = -4\omega_r^2\hat{Q} - \frac{4\omega_r\xi_{sm}\eta^2}{\kappa^2 + (\tilde{\Delta} + \xi\hat{q} - \xi_{sm}\hat{Q})^2}. \quad (7)$$

The corresponding effective Hamiltonian is described as $\hat{H}_{eff} = \hat{K} + \hat{V}$, where, $\hat{K} = \hat{p}^2/2$, here, $\hbar = 1$ is dimensionless Planck's constant. The potential \hat{V} is governed by Eq. (7). We assume that for a weak coupling the moving end mirror behaves like harmonic oscillator with frequency ω_m and $q = q_0 \cos(\omega_m t)$, where, q_0 is the maximum displacement from mean position. We introduce some dimensionless parameters defined as, $\gamma = 4\omega_r/\omega_m$, $\beta = \eta^2/\kappa^2$, $\mu = \Delta/\kappa$, $\mu_1 = \xi_{sm}/\kappa$, $\lambda = \frac{\xi_{sm}}{\xi}q_0$ and dimensionless time, $4\tau = \omega_m t$. Hence, from Eq. (7) we get,

$$\hat{V} = \frac{d\hat{Q}}{d\tau} = \frac{1}{2}\hat{Q}^2 + \int \frac{4\gamma\xi\beta/\omega_m}{1 + [\mu - \mu_1\{\hat{Q} - \lambda \cos(4\tau)\}]^2} dQ. \quad (8)$$

Now, we write the Hamiltonian as,

$$\hat{H}_{eff} = -\frac{1}{2}\frac{\partial^2}{\partial x^2} + \frac{1}{2}\hat{Q}^2 + \int \frac{4\gamma\xi\beta/\omega_m}{1 + [\mu - \mu_1\{\hat{Q} - \lambda \cos(4\tau)\}]^2} dQ. \quad (9)$$

By using transformation $\hat{X} = \hat{Q} - \lambda \cos(4\tau)$, we find an effective Hamiltonian for the condensate, that is,

$$\hat{H}_{eff} = \frac{1}{2}\hat{P}^2 + \frac{1}{2}\hat{X}^2 + \hat{X}\lambda_{eff}\cos(4\tau) - \frac{\gamma_m\beta}{\mu_1}\arctan(\mu - \mu_1\hat{X}), \quad (10)$$

where, $\gamma_m = \frac{4\xi}{\gamma\omega_m}$ and $\lambda_{eff} = (1 + \frac{32}{\gamma^2})\lambda$ is the effective modulation.

In our later work we consider the power of external field $P = 0.0164mW$ with frequency $\omega_p = 3.8 \times 2\pi \times 10^{14}Hz$ and wave length $\lambda_p = 780nm$. Coupling of external field and intra-cavity field is $\eta = 18.4 \times 2\pi MHz$ and frequency of intra-cavity field is considered $\omega_c = 15.3 \times 2\pi \times 10^{14}Hz$ which produces recoil of $\omega_r = 3.8 \times 2\pi kHz$ in atoms placed in cavity of length $l = 1.25 \times 10^{-4}m$ and having decay rate $\kappa = 1.3 \times 2\pi MHz$. Moving end mirror of cavity should be perfect reflector that oscillates with a frequency $\omega_m = 15.2 \times 2\pi kHz$. The mirror-field and condensate-field coupling strengths are, respectively, $\xi = 14.39KHz$ and $\xi_{sm} = 15.07MHz$. Detuning of the system is taken as $\Delta = \Delta_c + \frac{U_0 N}{2} = 0.52 \times 2\pi MHz$, where vacuum Rabi frequency of the system is $U_0 = 3.1 \times 2\pi MHz$ and number of ultra cold atoms placed in the BEC-optomechanical system are $N = 2.8 \times 10^4$ [2, 26–29].

IV. DYNAMICAL LOCALIZATION OF THE CONDENSATE

The quantum dynamics of dilute BEC is explored by evolving a Gaussian material wave packet, $\Psi(X)$, defined at $\tau = 0$ with, ΔX as its initial dispersion in the position space and ΔP corresponding to its initial dispersion in the momentum space.

Dynamics of the condensate is shown in Fig-1. Here, Fig-1(a) shows classical and quantum dispersion in momentum space as a function of time. Initially, the classical and quantum dispersion in momentum space follows the classical diffusion law but after quantum break time, quantum dispersion of the material wave packet saturates and oscillates around a mean value while, classical dispersion increases continuously with time, following t^α law, where $\alpha = 0.61$ showing anomalous diffusion in classical domain. Similarly, from Fig-1(b), we note that quantum dispersion in position space saturates after quantum break time and fluctuates around average value while, classical dispersion in position space that shows anomalous diffusion as well.

Here, Fig.-1(d,e) show classical and quantum time averaged probability distributions of BEC both in momentum and in position coordinates, respectively, for modulation amplitude $\lambda_{eff} = 1.05 \times 10^{-5}m$. We calculate probabilities in momentum coordinate $W(P) = |\Psi(P)|^2$ and position coordinate $W(X) = |\Psi(X)|^2$ after an evolution time $t = 4.19 \times 10^{-2}sec$. From the numerical results, we observe that the classical probability distribution in momentum and in position space are broader than their quantum mechanical counterpart. In contrast quantum

mechanical probability distributions are maximum at the points where the matter wave was initially placed and as we traverse the regions away from the initial mean values the probability of finding the matter wave both in momentum and in position space decreases. The mixed phase space with chaotic and regular regions appear due to the presence of modulated end-mirror that modifies the evolution of the condensate in effective nonlinear potential seen by the condensate in the cavity, as shown in Fig-1(f).

As probability distributions are marginal distributions of phase space, in quantum mechanical probability distributions the peak positions both in momentum and in position coordinates correspond to the underlying nonlinear resonances in the Poincare surface of section. Maximum fraction of the condensate is trapped with momentum in the range -3×10^{-27} to $3 \times 10^{-27}kg\ m/sec$ and in the position space $-3 \times 10^{-5}m$ to $3 \times 10^{-5}m$ because of regular regions in this domain as shown in Fig-1(f). In momentum distribution, peak at $P \sim 1.4 \times 10^{-30}kg\ m/sec$ corresponds to the regular region at same momentum value. Similarly, in position space distribution peaks at $X \sim -6.2 \times 10^{-6}$ and $X \sim 6.5 \times 10^{-6}$ corresponds to the regular regions appearing in phase space.

The part of the wave packet which is not in regular region experiences exponential decay which indicates that the probability of finding the condensate decreases exponentially in the regions away from the classical resonances. Maximum probability of finding the condensate is near the primary resonance as it originates initially from there. The exponential decay of distribution is one of the fundamental evidence of dynamical localization.

Fig-1(c) shows mean quantum mechanical energy $\langle H \rangle$ of the condensate as a function of time for $\lambda_{eff} = 1.05 \times 10^{-5}m$. The mean energy of the condensate shows very small fluctuation around a constant value and shows quantum recurrences as a function of time.

The consequence of dynamical localization in position and momentum space becomes prominent as we study the spatio-temporal dynamics of the condensate, presented in Fig-2. We show space-time dynamics in momentum space both in quantum mechanical and classical space, respectively, in Fig. 2(a) and 2(b). Whereas, we plot space-time dynamics in position space both quantum mechanically and classically, respectively, in Fig. 2(c) and 2(d). As the time evolves classical distributions both in momentum space and in position space melt down and spread over the entire available space with maximum probability in the resonances. On the other hand, quantum mechanical probability distributions in momentum space and in position space initially follow classical behavior, however, beyond quantum break time localization limits the spread. The maximum probability of finding the material wave packet stays around the nonlinear resonances. The material wave packet tunnels to other resonances which provide the exponential decay as shown in Fig. 1(d,e), therefore probability of finding the condensate in neighboring resonances increases with time.

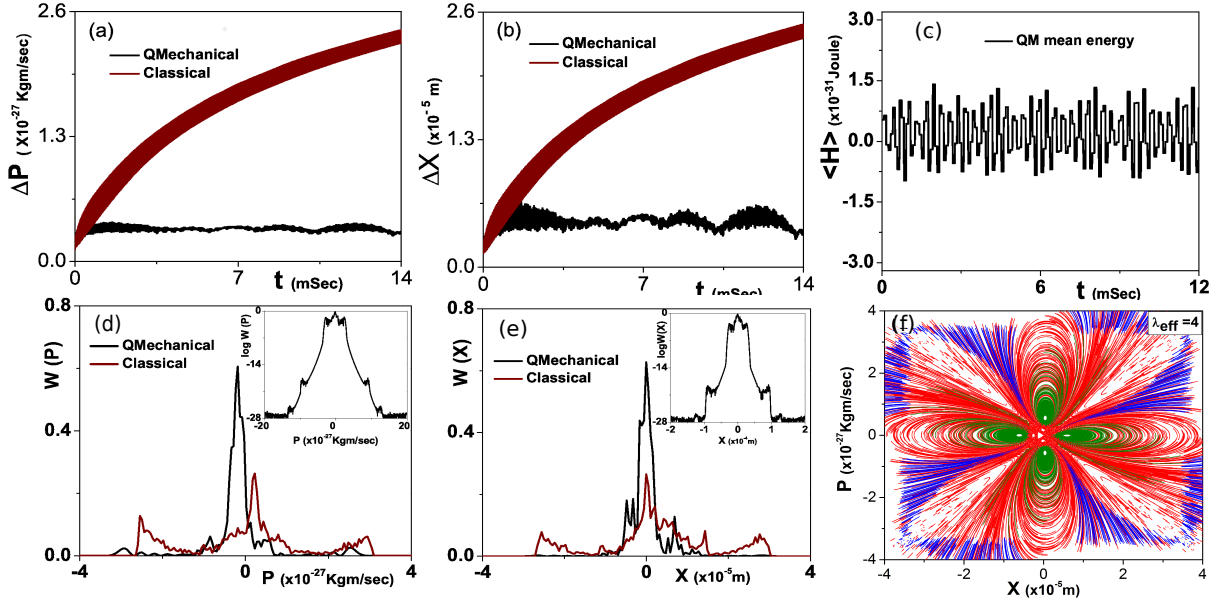


FIG. 1: (a) shows dispersion Δp in momentum space and (b) shows dispersion Δx in position space vs time for fixed modulation and gives comparison in quantum mechanical and classical behavior. (c) Mean energy of the condensate as a function of time. (d) Classical and quantum mechanical probability distribution in momentum space. (e) Classical and quantum mechanical probability distribution in position space of condensate for fixed time $t = 4.19 \times 10^{-2} \text{ sec}$. (f) Phase Space have initial distribution from -4 to 4 both in position space $P \times 10^{-26} \text{ kgm/sec}$ and momentum space $X \times 10^{-5} \text{ m}$. In all these figures modulation $\lambda_{\text{eff}} = 1.05 \times 10^{-5} \text{ m}$. Moreover, $\mu = -0.4$, $\mu_1 = 2$, $\beta = 1.8$ and $\gamma_m = 0.6034$.

V. EFFECTS OF MODULATION

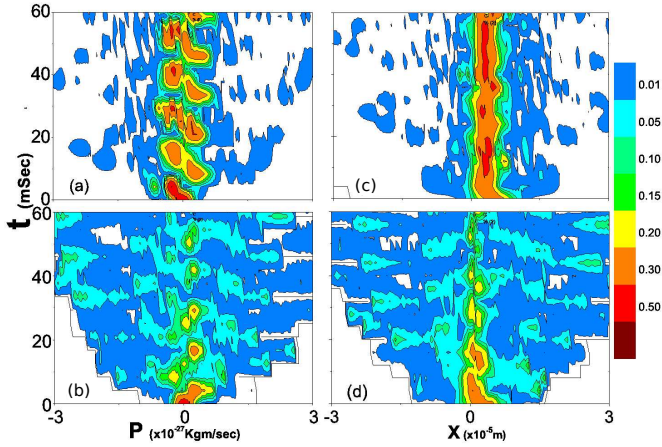


FIG. 2: Classical and quantum mechanical probability distribution versus time. (a) Quantum mechanical distribution in momentum space and (b) in position space. (c) Classical distribution in momentum space and (d) in position space. The modulation is fixed as $\lambda_{\text{eff}} = 1.05 \times 10^{-5} \text{ m}$. The remaining parameters are same as in Fig-1.

We numerically study the classical dispersion and quantum dispersion of the condensate both in momentum space Fig-3(a) and in position space Fig-3(b) as a function of modulation strength for a fixed time. For a small value of modulation classical and quantum dispersions deviate slightly both in position and in momentum space. As we increase the modulation in the system, momentum and position dispersions show contrasting behavior in classical and in quantum mechanical domain. In classical dynamics dispersion both in position space and in momentum space increases while, quantum dispersion displays saturation. The quantum dispersion manifests periodic oscillations in momentum space and in position space. At the minima of these oscillations we observe strong localization at particular modulation values where the difference between classical dispersion and quantum mechanical dispersion is maximum. As the value of rescaled Planck's constant, \hbar reduces, the time evolution of the quantum dispersion both in position and momentum space approaches to classical dispersion and periodic oscillation in the quantum mechanical dispersion vanish as well, hence, the periodic behavior is strictly quantum phenomena which may display quantum revivals in dynamical systems.

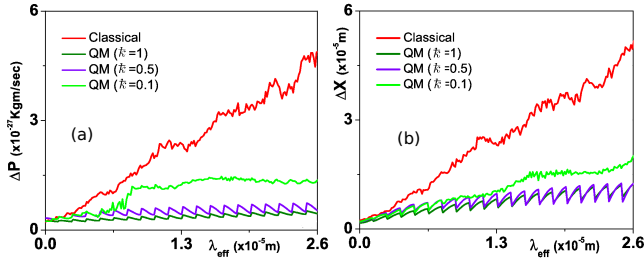


FIG. 3: Left figure shows classical and quantum dispersion in momentum space and right figure shows classical and quantum dispersion in position space as function of modulation. These dispersion in momentum and position space are observed after an evolution time $t = 2.09 \times 10^{-2} \text{ sec}$. The other parameters are same as in Fig. 1.

VI. CONCLUSION

In this contribution we study the dynamics of a condensed atoms in an opto-mechanical system where it is

coupled to the moving end mirror through the cavity field and displays dynamically localization both in position and momentum space. A contrast between classical and quantum dynamics is the evidence of the existence of dynamical localization and its presence is the signature of quantum chaos in a dynamical system. This behavior is different from the dynamical localization of ultra-cold atoms in modulated optical field where localization is observed only in momentum space [20]. Spatio-temporal dynamics of condensate in position and momentum space confirm our finding as well. We have also calculated the dispersion in position and momentum space as a function of modulation for fixed time. The dynamical localization phenomenon is realizable experimentally in position and in momentum space by using presently available experimental parameters.

-
- [1] T. J. Kippenberg and K. J. Vahala, *Science* **321**, 1172 (2008).
 - [2] F. Brennecke, S. Ritter, T. Donner, and T. Esslinger, *Science* **322**, 235 (2008).
 - [3] A. D. O'Connell et. al, *Nature* **464**, 697 (2010).
 - [4] J. D. Teufel et. al, *Nature* **475**, 359 (2011).
 - [5] J. Chan et. al, *Nature* **478**, 89 (2011).
 - [6] S. Groblacher, K. Hammerer, M.R. Vanner, and M. Aspelmeyer, *Nature (London)* **460**, 724 (2009).
 - [7] J. D. Teufel, D. Li, M. S. Allman, K. Cicak, A. J. Sirois, J. D. Whittaker, and R. W. Simmonds, *Nature (London)* **471**, 204 (2011).
 - [8] E. Verhagen, S. Deleglise, S. Weis, A. Schliesser, and T. J. Kippenberg, *Nature (London)* **482**, 63 (2012).
 - [9] V. Braginsky and S. P. Vyatchanin, *Phys. Lett. A* **293**, 328 (2002).
 - [10] D. Rugar et al., *Nature (London)*, **430**, 329 (2004).
 - [11] M. Eichenfield et al., *Nature* **462**, 78, (2012).
 - [12] K. Zhang, W. Chen, M. Bhattacharya, and P. Meystre, *Phys. Rev. A* **81**, 013802 (2010).
 - [13] Ying-Dan Wang and A. A. Clerk, *Phys. Rev. Lett.* **108**, 153603, (2012).
 - [14] S. Singh et al., *Phys. Rev. A* **86**, 021801, (2012).
 - [15] M. Asjad, and F. Saif, *Phys. Rev. A* **84**, 033606 (2011).
 - [16] L. F. Buchmann et al., *Phys. Rev. Lett.* **108**, 210403 (2012).
 - [17] R. Blumel et al., *Nature (London)* **334**, 309 (1988); M. Moore, R. Blumel, *Phys. Rev. A* **48**, 3082 (1993).
 - [18] S. Fishman, Grepel, D. R., Prange, R. E., *Phys. Rev. Lett.* **49**, 509 (1982).
 - [19] R. Blümel et al. *Phys. Rev. A* **44**, 4521 (1991).
 - [20] F. L. Moore et al., *Phys. Rev. Lett.* **73**, 2974 (1994).
 - [21] P. J. Bardroff et al., *Phys. Rev. Lett.* **74**, 3959 (1995).
 - [22] A. Schelle, Dominique Delande, and Andreas Buchleitner *Phys. Rev. Lett.* **102**, 183001 (2009).
 - [23] J. Esteve et al., *Nature (London)* **455**, 1216 (2008); F. Brennecke, et al., *ibid*, **450**, 268 (2007).
 - [24] F. Brennecke, S. Ritter, T. Donner, T. Esslinger, *Science* **322**, 235 (2008).
 - [25] C. K. Law, *Phys. Rev. A* **51**, 2537 (1995).
 - [26] T. Carmon, H. Rokhsari, L. Yang, T. J. Kippenberg, and K. J. Vahala, *Phys. Rev. Lett.* **94**, 223902 (2005).
 - [27] T. Carmon, M. C. Cross, and K. J. Vahala, *Phys. Rev. Lett.* **98**, 167203 (2007).
 - [28] A. Öttl, S. Ritter, M. Khl, and T. Esslinger *Rev. Sci. Instrum.* **77**, 063118 (2006).
 - [29] F. Brennecke, T. Donner, S. Ritter, T. Bourdel, M. Kohl, T. Esslinger, *Nature (London)* **450**, 268 (2007).
 - [30] C. W. Gardiner, *Quantum Noise* (Berlin, Springer, 1991).
 - [31] M. Paternostro, S. Gigan, M. S. Kim, F. Blaser, H. R. Böhm, and M. Aspelmeyer, *New Journal of Physics* **8**, 107 (2006).
 - [32] T. J. Kippenberg and K. J. Vahala, *Optics Express*, 17172 (2007).